

## Relative Sensitivity of XEDS vs EELS in the AEM

*D. Huber<sup>1</sup>, H.L. Fraser<sup>1</sup>, D.O. Klenov<sup>2</sup>, H.S. von Harrach<sup>2</sup>, N. J. Zaluzec<sup>3</sup>*

<sup>1</sup>*Dept of Materials Science & CAMM, The Ohio State University, Columbus OH, USA*

<sup>2</sup>*FEI Company, Achtseweg Noord 5, 5600 KA Eindhoven, The Netherlands*

<sup>3</sup>*Electron Microscopy Center, Mat. Science Div, Argonne National Laboratory, Argonne IL, USA*

Traditionally, electron energy loss spectroscopy (EELS) has been viewed as one of the most efficient means for microanalytical measurements in the analytical electron microscope. This view is based not only upon the physics of the signal generation process but also due to EELS' relatively high geometrical signal collection efficiency relative to that encountered with x-ray energy dispersive spectrometers (XEDS). Recent developments in silicon drift detectors (SDDs) has created a new generation of large solid angle spectrometers, which are challenging this view [1-3].

To assess the merits of these two techniques, simultaneous XEDS and EELS data sets were measured as a function of thickness using state-of-the-art spectrometer systems on a FEI Tecnai Osiris system. This instrument was equipped with a Super-X high solid angle XEDS system having a nominal solid angle of 0.9 sr, and a FS-1 EEL spectrometer. The specimen was an ion-milled single crystal of stoichiometric NiO, held in a double tilt Be analytical TEM stage that was slightly tilted to achieve non-channelling conditions. Measurements were made at 200 kV in STEM mode using a nominal probe diameter of 0.5 nm and a probe current of ~ 0.9 nA. The probe illumination and collection solid angles were 9 and 18 mR respectively.

Figures 1 and 2 show a selection of spectra taken from a series of 100 data points made as a function of thickness ranging from  $t/\lambda = 0.11$  to 1.75 (~ 11-177 nm) thick. In both data sets we can observe the effects of thickness. In EELS, it is manifest by the onset of multiple scattering, while in XEDS, it is evidenced by onset of x-ray absorption for the low energy lines. Figures 3 and 4 plot the variation in Edge/Background (EELS) and Peak/Background (XEDS) and the relative intensity ratios, respectively for this thickness range. For EELS data, the edge integration windows were set at 75 eV, while for XEDS the full peak width was used. The background windows were chosen to match the signal windows. These figures dramatically illustrate the severe degradation of the Edge/Bgnd for EELS due to multiple inelastic scattering, and for the first time we demonstrate that when suitable x-ray detector technology is employed that the sensitivity of XEDS, as manifest in the P/B ratio not only competes, but for real world samples, out performs EELS, particularly when  $t/\lambda > 0.5$ .

Additional analysis is in progress to assess the formalism for quantitative analysis in XEDS, particularly in the case of multiple XEDS detectors arranged symmetrically around the specimen as exists in the Tecnai Osiris Super-X geometry.

### References

- [1] Zaluzec, N.J. "Innovative Instrumentation for Analysis of Nanoparticles: The  $\pi$  Steradian Detector", *Microscopy-Today*, 17, #4, 56-59 July 2009, doi: 10.1017/S1551929509000224
- [2] Zaluzec, N.J. "Detector Solid Angle Calculations for X-ray Energy Dispersive Spectrometry" *Microsc. Microanal.* 15, 93-98, 2009 doi:10.1017/S1431927609090217
- [3] H.S. von Harrach, P. Dona, B. Freitag, H. Soltau, A. Niculae & M. Rohde *Microsc Microanal* 15(Suppl2), 208-9 2009
- [4] This work was supported in part by the US DOE Office of Science, Contract DE-AC02-06CH11357 at ANL.

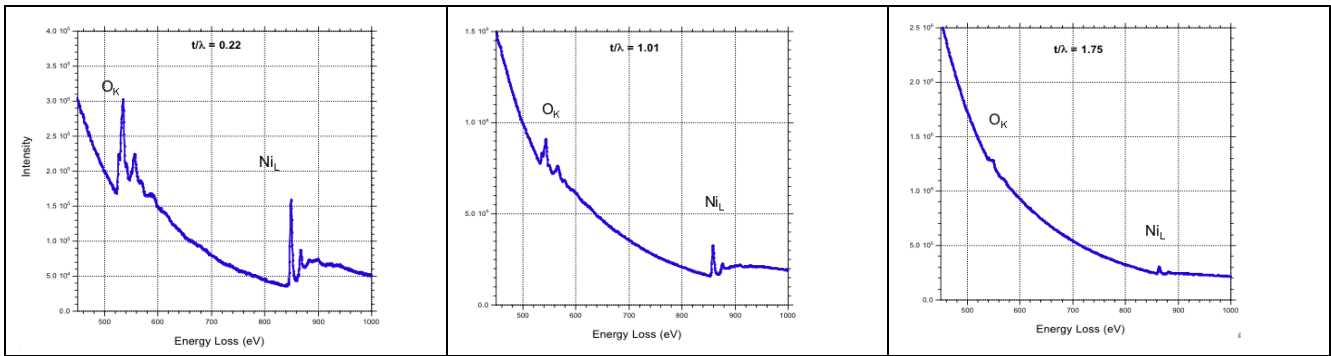


Figure 1.) Variation of EELS spectra as a function of  $t/\lambda$  .

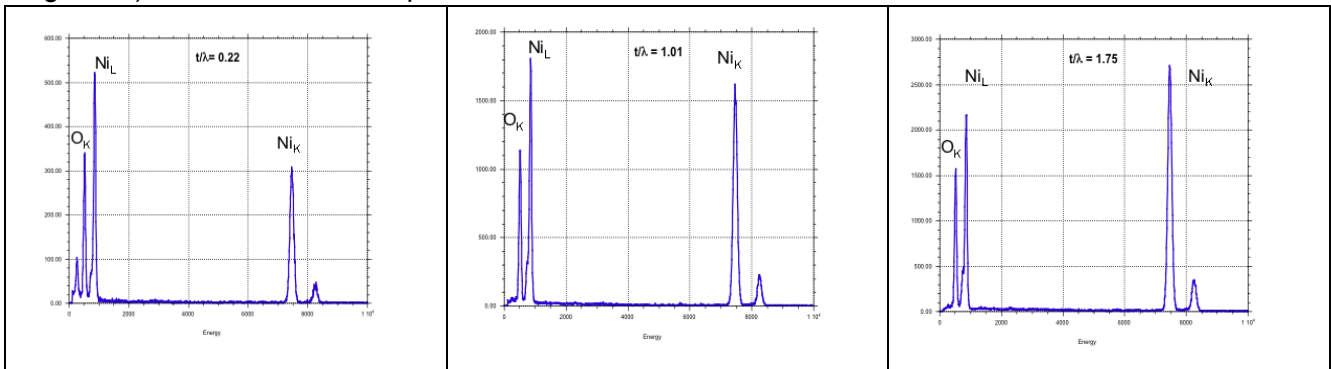


Figure 2.) Variation of XEDS spectra as a function of  $t/\lambda$  .

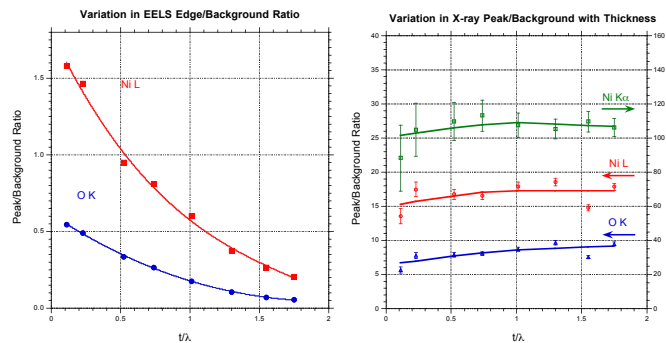


Figure 3.) Variation in the Edge/Background and Peak/Background Ratio as a function of  $t/\lambda$ . Note the rapid fall of the E/B Ratio for EELS while the P/B for XEDS is nearly constant.

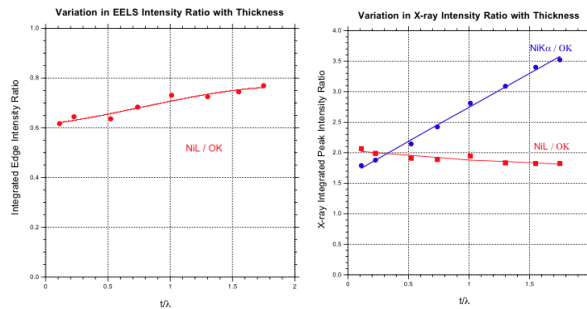


Figure 4.) Variation in the Relative Intensity Ratios as a function of  $t/\lambda$ .